



UNIVERSITY OF LEEDS

This is a repository copy of *Extending enzyme molecular recognition with an expanded amino acid alphabet*.

White Rose Research Online URL for this paper:
<http://eprints.whiterose.ac.uk/111212/>

Version: Accepted Version

Article:

Windle, CL, Simmons, KJ orcid.org/0000-0003-4846-9097, Ault, JR orcid.org/0000-0002-5131-438X et al. (4 more authors) (2017) Extending enzyme molecular recognition with an expanded amino acid alphabet. *Proceedings of the National Academy of Sciences*, 114 (10). pp. 2610-2615. ISSN 1091-6490

<https://doi.org/10.1073/pnas.1616816114>

© 2017, PNAS. This is an author produced version of a paper published in *Proceedings of the National Academy of Sciences*. Uploaded in accordance with the publisher's self-archiving policy. In order to comply with the publisher requirements the University does not require the author to sign a non-exclusive licence for this paper.

Reuse

Items deposited in White Rose Research Online are protected by copyright, with all rights reserved unless indicated otherwise. They may be downloaded and/or printed for private study, or other acts as permitted by national copyright laws. The publisher or other rights holders may allow further reproduction and re-use of the full text version. This is indicated by the licence information on the White Rose Research Online record for the item.

Takedown

If you consider content in White Rose Research Online to be in breach of UK law, please notify us by emailing eprints@whiterose.ac.uk including the URL of the record and the reason for the withdrawal request.



eprints@whiterose.ac.uk
<https://eprints.whiterose.ac.uk/>

Extending enzyme molecular recognition with an expanded amino acid alphabet.

Short title: Aldolase substrate specificity with Ncas

Claire L Windle^{1,2}, Katie Simmons^{1,3}, James R Ault^{1,2}, Chi H Trinh^{1,2}, Adam Nelson*^{1,3}, Arwen R Pearson^{1,4}, Alan Berry*^{1,2}

¹Astbury Centre for Structural Molecular Biology, University of Leeds, Leeds, LS2 9JT, UK;

²School of Molecular and Cellular Biology, University of Leeds, Leeds, LS2 9JT, UK; ³School of Chemistry, University of Leeds, Leeds, LS2 9JT, UK; ⁴Current address Hamburg Centre for Ultrafast Imaging & Institute for Nanostructure and Solid State Physics, Universität Hamburg, Hamburg 22761, Germany

Classification: BIOLOGICAL SCIENCES: Biochemistry

**Corresponding authors:*

Prof Alan Berry, ¹Astbury Centre for Structural Molecular Biology, University of Leeds, Leeds, LS2 9JT, UK. +44 113 343 3158 a.berry@leeds.ac.uk, ORCID: 0000-0003-3502-0426

Prof Adam Nelson, School of Chemistry, University of Leeds, Leeds, LS2 9JT, UK. +44 113 343 6502 a.s.nelson@leeds.ac.uk, ORCID: 0000-0003-3886-363X

ORCID Numbers: Berry: 0000-0003-3502-0426; Nelson: 0000-0003-3886-363X; Ault: 0000-0002-5131-438X; Simmons: 0000-0003-4846-9097; Trinh: 0000-0002-5087-5011; Pearson: 0000-0001-8499-7490; Windle: 0000-0002-4226-3832

Abstract

Natural enzymes are constructed from the twenty proteogenic amino acids, which may then require post-translational modification or the recruitment of coenzymes or metal ions to achieve catalytic function. Here, we demonstrate that expansion of the alphabet of amino acids can also enable the properties of enzymes to be extended. A chemical mutagenesis strategy allowed a wide range of non-canonical amino acids to be systematically incorporated throughout an active site to alter enzymic substrate specificity. Specifically, 13 different non-canonical side chains were incorporated at 12 different positions within the active site of *N*-acetylneuraminic acid lyase (NAL), and the resulting chemically-modified enzymes were screened for activity with a range of aldehyde substrates. A modified enzyme containing a 2,3-dihydroxypropyl cysteine at position 190 was identified that had significantly increased activity for the aldol reaction of erythrose with pyruvate compared with the wild-type enzyme. Kinetic investigation of a saturation library of the canonical amino acids at the same position showed that this increased activity was not achievable with any of the 20 proteogenic amino acids. Structural and modelling studies revealed that the unique shape and functionality of the non-canonical side chain enabled the active site to be remodelled to enable more efficient stabilisation of the transition state of the reaction. The ability to exploit an expanded amino acid alphabet can thus heighten the ambitions of protein engineers wishing to develop enzymes with new catalytic properties.

Keywords: Protein engineering, aldolases, chemical modification

Significance statement

The remarkable power of enzymes as catalysts is derived from the precise spatial positioning of amino acids as a result of a polypeptide folding into its native, active fold. Protein engineers have a wide arsenal of tools available to alter the properties of enzymes but, until recently, have been limited to replacement of amino acids with one of the other naturally occurring proteogenic amino acids. Here we describe a protein engineering approach to introduce a non-canonical amino acid that results in altered substrate specificity of an aldolase to produce a novel activity that cannot be achieved by simple substitution with any of the canonical amino acids.

\body

Introduction

Enzymes are phenomenally powerful catalysts that increase reaction rates by up to 10^{18} -fold (1, 2), and a new era of enzyme applications has been opened by the advancement of protein engineering and directed evolution to provide new, or improved, enzymes for industrial biocatalysis. Enzymes are attractive catalysts because they are highly selective, carrying out regio-, chemo- and stereo-selective reactions that are challenging for conventional chemistry. Moreover, enzymes are efficient catalysts, function under mild conditions with relatively non-toxic reagents, and enable the production of relatively pure products, minimising waste generation. In recent years, there has been much success in engineering enzymes for desired reactions (3-5) using methods such as rational protein engineering (6-8), directed evolution (9-11) and, most recently, computational enzyme design (12-15).

Enzymes found in Nature achieve catalysis using active sites generally composed of only 20 canonical amino acids, which are encoded at the genetic level, plus the rarer selenocysteine and 1-pyrrolysine. However, many enzymes also rely on one or more of 27 small organic cofactor molecules and/or 13 metal ions for their function (16). In addition, in some cases, Nature has exploited non-canonical amino acids (Nca) in catalysis to extend its catalytic repertoire: for example, the quinones TPQ, LTQ, TTQ and CTQ respectively in amine oxidase, lysyl oxidase, methylamine dehydrogenase and quinohemoprotein amine dehydrogenase (17); a pyruvoyl group in some histidine, arginine, aspartate and *S*-adenosylmethionine decarboxylases (18); formyl glycine residues in Type I sulfatases (19); and 4-methylideneimidazole-5-one (MIO) in ammonia lyases and 2,3-aminomutases (20). These Ncas are vital for catalysis and arise through post-translational modifications of the polypeptide chain (21, 22) allowing access to chemistries not otherwise provided by the 20 proteogenic amino acids.

Technologies for the protein engineer to incorporate Ncas into proteins at specifically chosen sites, either by genetic means (23-25) or by chemical modification (26, 27) have recently been developed. These approaches are powerful, since, unlike traditional protein engineering with the 20 canonical amino acids, protein engineering with Ncas has almost unlimited novel side-chain structures and chemistries from which to choose. This ability has been exploited to increase the stability of leucine-zipper peptides by replacing leucines with trifluoroleucine (Tfl) while maintaining the DNA-binding functions (28). Moreover, by screening random libraries with a sense codon global substitution method to replace Leu with Tfl, a mutant Tfl-containing enzyme with enhanced thermal stability (29) and a mutant Tfl-containing GFP with increased fluorescence intensity (30) were obtained. Incorporation of Ncas has also been used to generate a novel metalloenzyme by the *in vivo* incorporation of metal-binding Ncas into an active site (31). Furthermore, the efficiency of phosphotriesterase with the substrate paraoxon was improved by replacement of Tyr309 with the Nca L-(7-hydroxycoumarin-4-yl) ethyl glycine (32), generating a 10-fold improvement of an already highly efficient enzyme.

A particular challenge is the engineering of new enzymes for carbon–carbon bond formation, for example aldolases (33), since these can increase molecular complexity and control the formation of new stereocentres. We have taken the opportunity to incorporate Ncas into an aldolase to search for new activities that are dependent on the distinctive properties of the introduced Nca. The genetic incorporation of Ncas encodes the Nca as an amber STOP codon which is read by an orthogonal tRNA / amino acyl tRNA synthetase (tRNAs) pair to introduce directly the Nca *in vivo* (25). However, this method becomes extremely laborious if the effect of many different Ncas is to be investigated, as new orthogonal tRNA/tRNAs pairs must be evolved for each Nca. We have instead used chemical mutagenesis to incorporate a diverse range of Ncas throughout the active site of an aldolase, prior to screening these variants for activity with new substrates. We demonstrate that using this approach we can alter the substrate specificity of the enzyme, and achieve levels of activity towards a new substrate that are otherwise unattainable by mutagenesis to any of the canonical amino acids.

Results

Production of modified enzymes

N-Acetyl neuraminic acid lyase (NAL) catalyses the aldol reaction of *N*-acetyl-D-mannosamine and pyruvate to form *N*-acetylneuraminic acid (Fig. 1, Panel A). The substrate specificity and stereochemistry of this enzyme is highly malleable through protein engineering and directed evolution (34, 35), and we have shown that an enzyme bearing the Nca γ -thialysine (2-aminoethyl cysteine) in place of the catalytic Lys-165 retains activity (36). Here we have explored the effect of introducing Ncas throughout the active site on the reaction catalysed.

Twelve residues in the active site of *S. aureus* NAL were selected as positions for Nca incorporation (Fig. 2). The chemical modification procedure to introduce the Nca relies on the conversion of a cysteine into dehydroalanine by a bis-alkylation / elimination sequence (27, 36), followed by Michael addition of a thiol to introduce the new Nca side-chain. The *S. aureus* NAL naturally contains no cysteines making it an ideal target protein for chemical introduction of Ncas (36). The residues chosen for modification were picked based on their proximity to the aldehyde substrate binding pocket in the previously solved structure of an *E. coli* NAL variant in complex with 4-epi *N*-acetylneuraminic acid (pdb 4BWL) (37) (Fig. 3). The equivalent positions in the *S. aureus* NAL based on structural alignment were then mutated into cysteine residues by site-directed mutagenesis, and expressed and purified as previously described (36). The Ncas were then incorporated by first converting the cysteine to dehydroalanine (Dha) using 2,5-dibromohexan-1,6-diamide and then Michael addition with 13 different thiols resulting in installation of 13 different Ncas at each of the 12 positions (27) (Fig. 2). The thiols chosen encompass a wide variety of non-canonical side chains, some mimicking elongated versions of canonical amino acids and some incorporating functionalities that are either absent or uncommon in the canonical amino acids. Incorporation was carried out on a small (2.5 mg) scale under denaturing conditions to ensure the cysteine residue was accessible for modification before the protein was refolded. This procedure was previously shown to generate active, modified, refolded enzyme (36). The conversions of Cys→Dha and Dha→Nca were both monitored by ESI mass spectrometry (Figs. S1 & S2).

Screening and activity

NAL is highly specific for its ketone donor (pyruvate), while accepting a range of aldehyde acceptors (38, 39). However the wild-type enzyme has a strong preference for longer aldehydes (38-40): C4 aldehydes are generally poorly accepted (38) and C3 aldehydes are not substrates (39). The differently modified enzymes at each of the positions in the polypeptide chain were screened in 96-well plates

for altered activity and specificity in condensing pyruvate with a range of aldehyde substrates with different lengths (C4 to C6), stereochemistry and functional groups (Fig. 2). Enzyme activity was assessed using a variation of the established thiobarbituric acid (TBA) assay (41). Aldol reaction of pyruvate with the aldehydes in Table 1 generates 2-oxo-4,5-dihydroxy (or 2-oxo-4-acetamido-5-hydroxy) carboxylic acids. Subsequent cleavage of these products with periodate generates 1,3-dicarbonyls that react with TBA to generate an intense pink chromophore which can be quantified at 550 nm. Absorbance at 550 nm for each well was measured after 16 hours condensation. The results were analysed by comparing activity of the wild-type (un-modified) NAL with that of the Nca-containing enzyme with the same aldehyde substrate. An example analysis (Fig. 4) shows the result of screening NAL enzymes bearing Ncas at position 190 against a range of aldehydes. While most modifications either generated enzymes with lower activity than the wild-type (blue, Fig. 4) or with the same level of activity (white), three modified enzymes had activities for the condensation of pyruvate with erythrose considerably greater than that of wild-type enzyme (purple). The improved enzymes had 2-hydroxypropyl cysteine (Hpc), 4-hydroxybutyl cysteine (Hbc) or 2,3-dihydroxypropyl cysteine (Dpc) at residue 190, with the Phe190Dpc enzyme having the greatest activity. Interestingly, all the active enzymes have hydroxylated Nca side-chains.

To confirm that Phe190Dpc NAL catalyses the aldol reaction of pyruvate with erythrose to generate 3-deoxy-2-heptulosonic acid (DHA) (Fig. 1, Panel B), a large scale reaction was incubated for 48 hours with Phe190Dpc NAL, and the resulting diastereomeric mixture of product (DHA) was purified by anion exchange chromatography. The 500 MHz ^1H , COSY and TOCSY NMR spectra (Fig. S3) were in agreement with reported data (42) for the expected product (DHA), and showed that a ~75:25 mixture of C4-configured products had been formed (Table S1).

Characterisation of Phe190Dpc NAL

To evaluate fully the switch in substrate specificity caused by the introduction of the Dpc side chain at position 190, full kinetic characterisation of the reactions involving both ManNAc and erythrose was carried out. A large quantity (~ 50 mg) of Phe190Dpc NAL was produced and was subjected to size exclusion chromatography to remove any incorrectly folded protein produced during the refolding stage of the modification process. Mass spectrometry (Fig. S1) showed that the modified enzyme had the expected molecular mass for Phe190Dpc NAL. Steady-state kinetic parameters ($k_{\text{cat(app)}}$ and $K_{\text{m(app)}}$ for aldehyde) were determined for wild-type and Phe190Dpc NAL using the TBA assay (41) (Table 1; Fig. S4).

The kinetic parameters of the wild-type enzyme with ManNAc as acceptor aldehyde were in agreement with published values (43). Substitution of Phe-190 with Dpc results in ~3-fold decrease in the specificity constant $k_{\text{cat}}/K_{\text{m}(\text{app})}$ for ManNAc as substrate compared with the wild-type enzyme and this is almost entirely due to a decrease in $k_{\text{cat}(\text{app})}$. However when erythrose acts as the aldehyde substrate, the replacement of Phe-190 with Dpc results in a ~10-fold increase in the $k_{\text{cat}}/K_{\text{m}(\text{app})}$ for erythrose, including a 15-fold increase in $k_{\text{cat}(\text{app})}$. Taken together these results demonstrate a switch in substrate specificity from ManNAc to erythrose of approximately 30-fold brought about by the incorporation of an Nca at position 190. Interestingly the Nca-containing enzyme is about 10-times more active ($k_{\text{cat}(\text{app})}$) with the new substrate (erythrose) than the wild-type enzyme with its natural substrate (ManNAc). These results demonstrate that by replacing a hydrophobic phenylalanine with a polar Nca, 2,3-dihydroxypropyl cysteine, a new enzyme capable of the condensation of short (C4) aldehydes with high levels of catalytic activity can be generated.

Saturation mutagenesis of residue 190

To compare the activity achieved by insertion of Dpc at residue 190 of NAL, with that achievable by any of the 20 canonical amino acids, a saturation library at position 190 was produced. All 19 variants were produced by site-directed mutagenesis, expressed and purified (36). Kinetic parameters were then determined for the saturation library in the same way as for the wild-type and Phe190Dpc enzymes. Fig. 5 shows that varying the canonical amino acid at position 190 of the *S. aureus* NAL resulted in small increases in the activity of the enzyme towards the reaction of pyruvate with erythrose. In contrast, insertion of Dpc at position 190 produced an enzyme that was about 5-times more active with erythrose (in terms of both $k_{\text{cat}(\text{app})}$ and $k_{\text{cat}}/K_{\text{m}(\text{app})}$) than the best canonical amino acid (Glu) (Fig. 5B). These data clearly highlight the benefits of exploring a widened chemical space with regards to broadening enzyme substrate specificity.

Structural characterisation

It was interesting that the slight changes in enzyme specificity brought about by site-directed mutagenesis to introduce other canonical amino acids at position 190 in *S. aureus* NAL were mainly derived from changes in the apparent K_{m} for the aldehyde substrate (Fig. 5B). In contrast, the specificity change brought about by the introduction of the non-canonical Dpc side-chain was largely generated by changes in $k_{\text{cat}(\text{app})}$ rather than $K_{\text{m}(\text{app})}$ (Table 1). To investigate further the specificity change, we determined the structure of the Phe190Dpc NAL in complex with pyruvate (PDB 5LKY). The enzyme structure was highly similar ($\text{RMSD}_{\text{C}\alpha\text{-all-chains}}$ 0.49 Å and $\text{RMSD}_{\text{C}\alpha\text{-monomer}}$ 0.17-0.20 Å) to the wild-type pyruvate complex (PDB 4AH7 (36)) except at the modified position and around residue 167.

Identical interactions between the enzyme and the pyruvate donor indicate that its binding is unaffected by the insertion of the Dpc side chain. Residue 190 is positioned towards the aldehyde-binding end of the active site and the electron density was modelled as a (2*R*)-2,3-dihydroxypropyl cysteine. It is notable that the Nca has a single (L) stereochemical configuration. It is highly unlikely that the Michael addition of racemic 2,3-dihydroxy propanethiol to the unfolded protein was stereocontrolled; rather, we hypothesise, as previously (36), that only one stereoisomer of the modified protein can re-fold correctly and is recovered after gel filtration.

The Dpc190 side-chain is positioned between Glu192 and Asp141 and points into the active site where it extends further (average $0.8 \text{ \AA} \pm 0.1 \text{ \AA}$ from all four subunits) into the active site than the corresponding phenylalanine in the wild-type structure. The non-canonical side chain exhibits a high degree of flexibility in the active site, adopting different conformations in all four subunits (Fig. S5). In subunit A, the Dpc side chain was modelled in two different conformations which resulted from a rotation around the C α -C β bond. In both subunits A and B, the hydroxyl groups of the Dpc side chain make hydrogen bond interactions to the side chains of Glu192 and Asp141 (Fig 6B). Another notable difference between wild-type and Phe190Dpc NAL was at the region 167-169. In the Phe190Dpc structure, the removal of the bulky hydrophobic phenylalanine allows the backbone chain containing residues Thr167, Ala168 and Pro169 to move closer to the catalytic Lys165 in the active site (Fig S6). This results in the C α of Thr167 in the Phe190Dpc structure being displaced on average $1.0 \text{ \AA} \pm 0.1 \text{ \AA}$ and adopting a different rotamer when compared to the wild-type structure (Fig. 6A & B, Fig S6). Previous QMMM modelling of the reaction mechanism of the *E. coli* NAL (37) has suggested that Thr167 binds to the aldehyde oxygen atom and helps to stabilise the transition state of the reaction. Unfortunately, we were unable to determine the crystal structure of the modified Phe190Dpc NAL with the reaction product DHA bound and so we turned to molecular modelling to try to elucidate the structural basis for the change of specificity.

Computational energy minimisation experiments were carried out on the Schiff bases formed between the product DHA and both the wild-type and Phe190Dpc NALs. The models revealed that, as expected, the DHA, being shorter than the natural substrate Neu5Ac, does not make the same interactions with Glu-192 of the enzyme (37) (Fig S8). Because of our finding that both 4*R*- and 4*S*-DHA were formed by Phe190Dpc NAL, both stereoisomers were modelled into the active sites. The minimisations revealed that C1-C3 of either C4 diastereoisomer of DHA were bound in the same way in both the wild-type and Phe190Dpc models. However there were significantly different interactions at the other end (C4-C7) of the product. Tyr252 lies slightly further from the product in both 4(*R*) and 4(*S*) DHA-Phe190Dpc NAL models, meaning that it can no longer hydrogen bond with the product C5

hydroxyl (~ 4.7 Å compared with 3.1 Å in the wild-type model) (Fig 6 C and D). In addition, Thr167 lies ~ 1.6 Å closer to the C4 hydroxyl of the product in the DHA-Phe190Dpc model than in the wild-type model: here, the difference in the preferred rotamer of Thr167 may enable better stabilisation of the enzyme transition state. Dpc does not interact directly with DHA in the Phe190Dpc model; it forms an entirely different network of interactions between the carboxylate side chains of Asp141 and Glu192 in the wild-type model. This brings the Dpc 3.0 Å closer to the product than the phenylalanine in the wild-type model (Fig S7). Thus, molecular modelling suggests that the newly introduced Dpc side chain at residue 190 alters the substrate specificity not by direct interaction with DHA, but rather by altering the conformation and interaction network in the active site resulting in better transition state stabilisation. This observation is entirely consistent with the kinetic data (Table 2) where the switch in substrate specificity measured by $k_{\text{cat}}/K_{\text{m(app)}}$ is almost entirely due to alterations in $k_{\text{cat(app)}}$ rather than in $K_{\text{m(app)}}$.

Discussion

Aldolases are an important class of biocatalysts which are finding increasing uses in the synthesis of complex compounds (33). They are particularly useful in that they can create two stereochemical centres during their reaction (34, 44-46) and that the reactions can be carried out in aqueous solvent without the use of protecting groups. However, the substrate specificity of natural aldolases often has to be engineered in order to produce enzymes with the required substrate specificity (33, 47). Rational protein engineering and directed evolution have been successful in addressing this problem, but the protein engineer is nonetheless fundamentally limited to alterations of amino acids to any of the other 19 canonical amino acids. The recent invention of methods to allow the incorporation of non-canonical amino acids into proteins, either by genetic incorporation or by chemical modification, has opened the way to explore wider areas of structure–activity space. Chemical modification methods have particular value since many different Ncas may be incorporated easily, enabling the function of the resulting variants to be explored. Here, we have shown that by utilising a non-canonical amino acid, it is possible not only to alter the aldehyde acceptor of the natural enzyme, but also to increase the activity with the altered substrate to rates that are unattainable with only the 20 proteogenic amino acids.

By modifying position 190 of the *S. aureus* NAL to a 2,3-dihydroxypropyl cysteine, the enzyme activity for the reaction of erythrose and pyruvate to form DHA (Fig. 1) has been significantly increased. A phosphorylated form of DHA (7-phospho DHA) is an important intermediate in the shikimate pathway for the biosynthesis of aromatic amino acids (48) and there has been much interest in the preparation of DHA, and other 3-deoxy-2-ulosonic acids, due to their potential as starter units for complex

oligosaccharide syntheses (42, 48-50). Our structural studies showed that the non-canonical amino acid is perfectly shaped and functionalised to interpose between Asp141 and Glu192; reducing the active site volume causing a remodelling of the active site to stabilise better the transition state of the DHA-producing reaction. In stark contrast, none of the canonical amino acids possess the required molecular characteristics in a single residue, demonstrating that Ncas can extend the ambitions of the protein engineer. Based on the data presented here, we envisage that advances in computational (12, 13) and (semi-)rational methods (6) for enzyme redesign, coupled with the development of recent powerful chemical mutagenesis methods (51) and the enormous variety of Ncas side chains and chemistries, will open the way to engineer enzymes with catalytic functions that are not found in Nature.

Materials and Methods

Further details may be found in Supporting Text.

Chemical modification using various different thiols

The conversion of the cysteine residues (introduced by site-directed mutagenesis) to dehydroalanine was carried out as previously described (36) using 2,5-dibromohexan-1,6-diamide synthesised as described (27). ESI-MS was used to check for complete conversion into the Nca-containing protein. Small scale (2.5 mg) modifications were used for the screening process. For detailed characterisation, large scale modifications (up to 50 mg) were performed. Modified enzymes were refolded by first dialysing into sodium phosphate buffer (50 mM, pH 7.4) containing urea (6 M) to remove excess modification reagents, followed by dialysis into buffer without urea to refold the enzyme (36). Large scale protein modifications were purified using size exclusion chromatography performed using an ÄKTA Prime purification system (GE Healthcare Life Sciences) with a Superdex S200 column. Protein (8 mg/mL, 5 mL) was injected onto the column which was run in Tris/HCl buffer (50 mM, pH 7.4) at 2 mL/min.

Screening using the thiobarbituric acid (TBA) assay

Modified enzymes were screened for aldol reaction activity with pyruvate and a variety of aldehydes. Reactions in 96 deep well plates contained pyruvate (100 μ L, final concentration 80 mM), aldehyde (100 μ L, final concentration 8 mM) and modified enzyme (50 μ L of 1.0 mg/mL (1.5 nmol)). Reactions were incubated for 16 hours at room temperature and activity was assessed by the TBA assay. Each reaction was oxidised by the addition of 11 μ L of sodium periodate (0.2 M in 9 M H₃PO₄) and incubated for 20 min at room temperature. Oxidation was terminated by the addition of 45 μ L of sodium arsenite

(10% w/v in 0.5 M Na₂SO₄ and 0.05 M H₂SO₄), and reactions were agitated until all brown discoloration had dissipated. 135 µL of TBA (0.6% w/v in 0.5 M NaSO₄) was added to each reaction and heated to 70 °C for 30 min. 100 µL samples of each reaction were transferred to a flat bottomed 96-well plate and the absorbance was read at 550 nm.

Synthesis of 3-deoxy-D-arabino-2-heptulopyranosonic acid (DHA)

Erythrose (500 mg, 4.2 mmol) and sodium pyruvate (2.29 g, 21 mmol) were dissolved in sodium phosphate buffer (50 mM pH 7.4 10 mL) and Phe190Dpc (0.8 mg) was added. The reaction was incubated at room temperature for a minimum of 48 hours before purification by anion exchange chromatography on AG1x8 resin (HCO₃⁻, 100-200 mesh). Product was eluted using a 0-0.4 M ammonium bicarbonate linear gradient (52). Fractions containing product were identified using the TBA assay on a 20 µL sample and were pooled, freeze dried and re-dissolved in D₂O before analysis by 500 MHz ¹H, COSY and TOCSY NMR spectroscopy.

Kinetic assays

Kinetic parameters were determined using the TBA assay. 100 µL reactions contained erythrose (0.8-15 mM) and pyruvate (80 mM). Reactions were initiated by the addition of 25 µL of enzyme (0.7 mg/mL; 0.5 nmol) and then incubated at room temperature for 1.5 hours. A 100 µL sample was taken from each reaction and stopped by the addition of 10 µL trichloroacetic acid (12 % w/v). Precipitated proteins were removed by centrifugation and samples were analysed. Under these conditions the rate of formation of product was linear over 90 minutes (Fig. S4) and the initial rate of the reaction was determined from the A_{550 nm} against a standard curve of *N*-acetylneuraminic acid. Reactions were analysed in duplicate and kinetic parameters were estimated by fitting to the Michaelis-Menten equation using non-linear regression analysis. Parameter values ± standard error of the fit are reported throughout.

Protein crystallisation, data collection and refinement

Crystallisation conditions were as previously described (36, 53). Diffraction data for the Phe190Dpc structure were collected from a single crystal at the Diamond Light Source macromolecular crystallography beam line I04-1 flash cooled to 100 K. Data processing and refinement were carried out as previously described (36). Coordinates and restraint library files for the 2, 3-dihydroxypropyl cysteine side chain (HET code P9S) were generated using the PRODRG (54) server and manually edited. The models were validated using the PDB validation server. Atomic coordinates and structure factors have been deposited into the Protein data Bank with the accession code 5LKY (Table S2).

Computational energy minimisations

Computational energy minimisations were carried out using the Schrodinger Small Molecule Discovery Suite (Schrödinger Release 2015-1: Maestro, Schrödinger, LLC, New York). Maestro was used to model the Schiff bases between the product DHA and the catalytic lysine of subunit B of the wild-type or Phe190Dpc NAL. Energy minimisation of the products formed was carried out using Macromodel with the OPLS_2005 force field (55) with water as solvent. All amino acid side chains within 6 Å of the product were allowed to minimise, as well as the product itself.

Acknowledgements

This work was supported by a BBSRC DTG PhD studentship (BB/F01614X/1 to CLW) and BBSRC grant (BB/N002091/1). Protein crystallisation and X-ray facilities were funded by BBSRC (BB/L015056/1) and the Wellcome trust (WT094232MA), respectively. Mass spectrometry was performed on a Xevo G2-XS & ACQUITY MClass UPLC funded by BBSRC (BB/M012573/1) and the nanoACQUITY HPLC was kindly donated by Waters UK, Manchester. The authors would like to thank Diamond Light Source for beamtime (proposal mx10305), and the staff of beamline I04-1 for assistance with data collection.

References

1. Lad C, Williams NH, & Wolfenden R (2003) The rate of hydrolysis of phosphomonoester dianions and the exceptional catalytic proficiencies of protein and inositol phosphatases. *Proc. Natl. Acad. Sci. U. S. A.* 100(10):5607-5610.
2. Stockbridge RB, Lewis CA, Jr., Yuan Y, & Wolfenden R (2010) Impact of temperature on the time required for the establishment of primordial biochemistry, and for the evolution of enzymes. *Proc. Natl. Acad. Sci. U. S. A.* 107(51):22102-22105.
3. Bornscheuer UT, *et al.* (2012) Engineering the third wave of biocatalysis. *Nature* 485(7397):185-194.
4. Jäckel C & Hilvert D (2010) Biocatalysts by evolution. *Curr. Opin. Biotechnol.* 21(6):753-759.
5. Davids T, Schmidt M, Bottcher D, & Bornscheuer UT (2013) Strategies for the discovery and engineering of enzymes for biocatalysis. *Curr. Opin. Chem. Biol.* 17(2):215-220.
6. Lutz S (2010) Beyond directed evolution-semi-rational protein engineering and design. *Curr. Opin. Biotechnol.* 21(6):734-743.
7. Baker P & Seah SYK (2012) Rational approaches for engineering novel functionalities in carbon-carbon bond forming enzymes. *Comput. Struct. Biotechnol. J.* 2(3):1-10.
8. Chica RA, Doucet N, & Pelletier JN (2005) Semi-rational approaches to engineering enzyme activity: combining the benefits of directed evolution and rational design. *Curr. Opin. Biotechnol.* 16(4):378-384.
9. Packer MS & Liu DR (2015) Methods for the directed evolution of proteins. *Nat. Rev. Genet.* 16(7):379-394.
10. Brustad EM & Arnold FH (2011) Optimizing non-natural protein function with directed evolution. *Curr. Opin. Chem. Biol.* 15(2):201-210.
11. Lane MD & Seelig B (2014) Advances in the directed evolution of proteins. *Curr. Opin. Chem. Biol.* 22:129-136.
12. Wijma HJ & Janssen DB (2013) Computational design gains momentum in enzyme catalysis engineering. *FEBS J.* 280(13):2948-2960.
13. Kries H, Blomberg R, & Hilvert D (2013) *De novo* enzymes by computational design. *Curr. Opin. Chem. Biol.* 17(2):221-228.
14. Huang PS, Boyken SE, & Baker D (2016) The coming of age of *de novo* protein design. *Nature* 537(7620):320-327.
15. Wijma HJ, *et al.* (2015) Enantioselective enzymes by computational design and *in silico* screening. *Angewandte Chemie-International Edition* 54(12):3726-3730.
16. Holliday GL, Fischer JD, Mitchell JB, & Thornton JM (2011) Characterizing the complexity of enzymes on the basis of their mechanisms and structures with a bio-computational analysis. *FEBS J.* 278(20):3835-3845.
17. Davidson VL (2011) Generation of protein-derived redox cofactors by post-translational modification. *Mol. Biosyst.* 7(1):29-37.
18. Bale S & Ealick SE (2010) Structural biology of S-adenosylmethionine decarboxylase. *Amino acids* 38(2):451-460.
19. Bojarova P & Williams SJ (2008) Sulfotransferases, sulfatases and formylglycine-generating enzymes: a sulfation fascination. *Curr. Opin. Chem. Biol.* 12(5):573-581.
20. Turner NJ (2011) Ammonia lyases and aminomutases as biocatalysts for the synthesis of alpha-amino and beta-amino acids. *Curr. Opin. Chem. Biol.* 15(2):234-240.
21. Yukl ET & Wilmot CM (2012) Cofactor biosynthesis through protein post-translational modification. *Curr. Opin. Chem. Biol.* 16(1-2):54-59.
22. Klinman JP & Bonnot F (2013) Intrigues and intricacies of the biosynthetic pathways for the enzymatic quinocofactors: PQQ, TTQ, CTQ, TPQ, and LTQ. *Chem. Rev.* 114(8):4343-4365.
23. Zhang WH, Otting G, & Jackson CJ (2013) Protein engineering with unnatural amino acids. *Curr. Opin. Struct. Biol.* 23(4):581-587.

24. Dumas A, Lercher L, Spicer CD, & Davis BG (2015) Designing logical codon reassignment - Expanding the chemistry in biology. *Chem. Sci* 6(1):50-69.
25. Young TS & Schultz PG (2010) Beyond the canonical 20 amino acids: expanding the genetic lexicon. *J. Biol. Chem.* 285(15):11039-11044.
26. Diaz-Rodriguez A & Davis BG (2011) Chemical modification in the creation of novel biocatalysts. *Curr. Opin. Chem. Biol.* 15(2):211-219.
27. Chalker JM, *et al.* (2011) Methods for converting cysteine to dehydroalanine on peptides and proteins. *Chemical Science* 2(9):1666-1676.
28. Tang Y, *et al.* (2001) Stabilization of coiled-coil peptide domains by introduction of trifluoroleucine. *Biochemistry* 40(9):2790-2796.
29. Montclare JK & Tirrell DA (2006) Evolving proteins of novel composition. *Angew. Chem. Int. Ed.* 118(27):4630-4633.
30. Yoo TH, Link AJ, & Tirrell DA (2007) Evolution of a fluorinated green fluorescent protein. *Proc Natl Acad Sci U S A* 104(35):13887-13890.
31. Drienovska I, Rioz-Martinez A, Draksharapu A, & Roelfes G (2015) Novel artificial metalloenzymes by *in vivo* incorporation of metal-binding unnatural amino acids. *Chemical Science* 6(1):770-776.
32. Ugwumba IN, *et al.* (2011) Improving a natural enzyme activity through incorporation of unnatural amino acids. *J. Am. Chem. Soc.* 133(2):326-333.
33. Windle CL, Muller M, Nelson A, & Berry A (2014) Engineering aldolases as biocatalysts. *Curr. Opin. Chem. Biol.* 19:25-33.
34. Williams GJ, Woodhall T, Farnsworth LM, Nelson A, & Berry A (2006) Creation of a pair of stereochemically complementary biocatalysts. *J. Am. Chem. Soc.* 128(50):16238-16247.
35. Williams GJ, Woodhall T, Nelson A, & Berry A (2005) Structure-guided saturation mutagenesis of N-acetylneuraminic acid lyase for the synthesis of sialic acid mimetics. *Protein Eng. Des. Sel.* 18(5):239-246.
36. Timms N, *et al.* (2013) Structural insights into the recovery of aldolase activity in N-acetylneuraminic acid lyase by replacement of the catalytically active lysine with gamma-thialysine by using a chemical mutagenesis strategy. *Chembiochem* 14(4):474-481.
37. Daniels AD, *et al.* (2014) Reaction Mechanism of N-acetylneuraminic acid lyase revealed by a combination of crystallography, QM/MM simulation, and mutagenesis. *ACS Chem. Biol.* 9(4):1025-1032.
38. Fitz W, Schwark J-R, & Wong C-H (1995) Aldotetroses and C(3)-modified aldohexoses as substrates for N-acetylneuraminic acid aldolase: A model for the explanation of the normal and the inversed stereoselectivity. *J. Org. Chem.* 60(12):3663-3670.
39. Kim MJ, Hennen WJ, Sweers HM, & Wong CH (1988) Enzymes in carbohydrate synthesis: N-acetylneuraminic acid aldolase catalyzed reactions and preparation of N-acetyl-2-deoxy-D-neuraminic acid derivatives. *J. Am. Chem. Soc.* 110(19):6481-6486.
40. Machajewski TD & Wong C-H (2000) The catalytic asymmetric aldol reaction. *Angew. Chem. Int. Ed.* 39(8):1352-1375.
41. Warren L (1959) Thiobarbituric acid assay of sialic acids. *J. Biol. Chem.* 234(8):1971-1975.
42. Hekking KFW, Moelands MAH, van Delft FL, & Rutjes FPJT (2006) An in-depth study on ring-closing metathesis of carbohydrate-derived alpha-alkoxyacrylates: Efficient syntheses of DAH, KDO, and 2-deoxy-beta-KDO. *J. Org. Chem.* 71(17):6444-6450.
43. Ferrero MA, Reglero A, FernandezLopez M, Ordas R, & RodriguezAparicio LB (1996) N-acetyl-D-neuraminic acid lyase generates the sialic acid for colominic acid biosynthesis in *Escherichia coli* K1. *Biochem. J.* 317:157-165.
44. Howard JK, Müller M, Berry A, & Nelson A (2016) An enantio- and diastereoselective chemoenzymatic synthesis of α -fluoro β -hydroxy carboxylic esters *Angew. Chem. Int. Ed.* 55:6767-6770.

45. Williams GJ, Domann S, Nelson A, & Berry A (2003) Modifying the stereochemical course of an enzyme-catalysed reaction by directed evolution. . *Proc. Natl. Acad. Sci. USA* 100:3143-3148.
46. Royer SF, *et al.* (2010) Structurally informed site-directed mutagenesis of a stereochemically promiscuous aldolase to afford stereochemically complementary biocatalysts. *J. Am. Chem. Soc* 132(33):11753-11758.
47. DeSantis G, *et al.* (2003) Structure-based mutagenesis approaches toward expanding the substrate specificity of D-2-deoxyribose-5-phosphate aldolase. *Bioorg. Med. Chem.* 11(1):43-52.
48. Dondoni A, Marra A, & Merino P (1994) Installation of the pyruvate unit in glycidic aldehydes via a Wittig olefination Michael addition sequence utilizing a thiazole-armed carbonyl ylid - a new stereoselective route to 3-deoxy-2-ulosonic acids and the total synthesis of DAH, KDN and 4-epi-KDN *J. Am. Chem. Soc* 116(8):3324-3336.
49. Pradhan TK, Lin CC, & Mong KKT (2013) Formal synthesis of 3-deoxy-D-manno-octulosonic acid (KDO) and 3-deoxy-D-arabino-2-heptulosonic acid (DAH). *Synlett* 24(2):219-222.
50. Enders D & Gasperi T (2007) Proline organocatalysis as a new tool for the asymmetric synthesis of ulosonic acid precursors. *Chem. Commun.* (1):88-90.
51. Wright TH, *et al.* (2016) Posttranslational mutagenesis: A chemical strategy for exploring protein side-chain diversity. *Science (New York, N.Y.)*.
52. Auge C & Gautheron-Le Narvor C (1997) *Preparative Carbohydrate Chemistry* (Marcel Dekker, INC, New York).
53. Campeotto I, *et al.* (2010) Structural insights into substrate specificity in variants of N-acetylneuraminic acid lyase produced by directed evolution. *J. Mol. Biol.* 404(1):56-69.
54. Schuttelkopf AW & van Aalten DMF (2004) PRODRG: a tool for high-throughput crystallography of protein-ligand complexes. *Acta Crystallogr. D Biol. Crystallogr.* 60:1355-1363.
55. Banks JL, *et al.* (2005) Integrated modeling program, applied chemical theory (IMPACT). *J. Comput. Chem.* 26(16):1752-1780.

Figure Legends

Figure 1. Substrates and products of wild-type and modified *N*-acetylneuraminic acid lyase (NAL).

A) The wild-type enzyme catalyses the aldol reaction of *N*-acetyl-D-mannosamine (ManNAc) with pyruvate to form *N*-acetylneuraminic acid (Neu5Ac). B) The aldol reaction of erythrose and pyruvate to form (4*R*, -5*S*, -6*R*) or (4*S*, -5*S*, -6*R*) 3-deoxy-2-heptulosonic acid (DHA) catalysed by the modified *S. aureus* NAL bearing the non-canonical amino acid dihydroxypropyl cysteine at position 190.

Figure 2. Amino acid positions modified, modifying thiols and screening substrates.

Cysteine residues were introduced individually into *S. aureus* NAL by site-directed mutagenesis at each position shown. After conversion into dehydroalanine, each position was modified separately with the thirteen thiols shown. The resulting enzymes were screened using the thiobarbituric acid assay for activity in condensing pyruvate with the aldehydes shown.

Figure 3. Identification of positions for chemical modification.

The crystal structure of the Y137A mutant of *E. coli* NAL in complex with *N*-acetylneuraminic acid (Neu5Ac) (PDB 4BWL) (35) was used to select sites at which to incorporate Ncas. Residues were selected based on proximity (<8 Å) to the position of the Neu5Ac substrate (dark purple), and were separately mutated to cysteine residues. Residues at these positions are conserved between the *E. coli* and *S. aureus* enzymes except for the following conservative changes (*E. coli* residue first): D170N, Y172F, Y190F I247L, V251I and F252Y.

Figure 4. Screening data for enzymes modified at position 190.

Overnight reactions of enzyme (0.2 mg; 5.8 nmol) with aldehyde (8 mM) and pyruvate (80 mM) were assayed using the TBA assay and the absorbance read at 550 nm. The difference in A_{550} between the reaction with the modified enzyme and the wild-type enzyme were calculated. Values below zero (modified enzyme is less active than wild-type) are blue with the intensity proportional to the activity difference. Values greater than zero (modified enzyme is more active than wild-type) are similarly coloured in pink. Modified enzymes are ranked by order of activity with pyruvate and erythrose.

Figure 5. Comparison of activities for the saturation library at position 190 against F190Dpc variant.

Activity of NAL variants bearing the 20 canonical amino acids at position 190 was measured using the TBA assay and compared with NAL bearing the Nca Dpc at position 190. Initial reaction rates were determined using the TBA assay under conditions where the time course of product formation is linear

(Fig. S4). Steady-state kinetic parameters were determined at a fixed pyruvate concentration of 80 mM and erythrose concentrations between 0.8 mM and 15 mM. Each reaction contained 18 μ g (0.52 nmol) of enzyme and were carried out in duplicate and data were fitted to the Michaelis-Menten equation. The fitted value \pm standard error of the fit is shown. A: comparison of k_{cat} values; B: steady-state parameters.

Figure 6. Structures and models of wild-type and modified NALs.

Structures of (A) wild-type (PDB 4AH7 (34)) and (B) Phe190Dpc (PDB 5LKY) NAL enzymes in complex with pyruvate were structurally aligned. Panel B shows the network of interactions that the Nca side chain Dpc forms with Asp141 and Glu192. Energy minimised models of product-Schiff base structures (illustrated with 4(S)-DHA) were generated using Maestro and are displayed from the same view. Panel C: wild-type NAL; panel D Phe190Dpc enzyme complex.

Fig 1

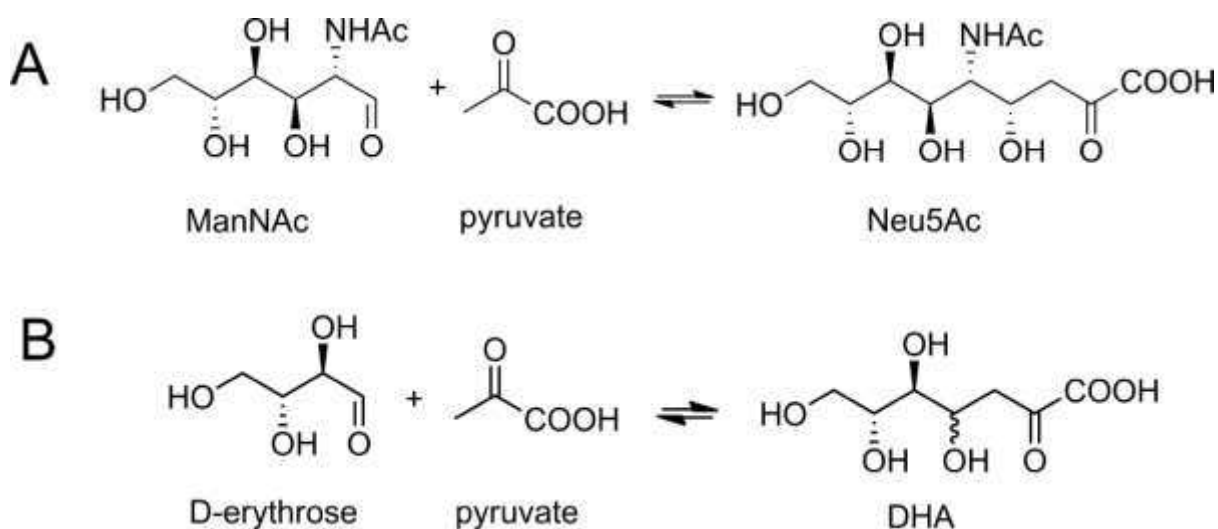


Fig 2

Cysteine variants	Thiols	Aldehydes								
L247C I251C		<table border="0"> <tr> <td></td> <td></td> <td></td> <td></td> </tr> <tr> <td></td> <td></td> <td></td> <td></td> </tr> </table>								
L142C F190C										
Y252C G207C										
E192C I139C										
F172C N170C										
T209C S208C										

Fig 3

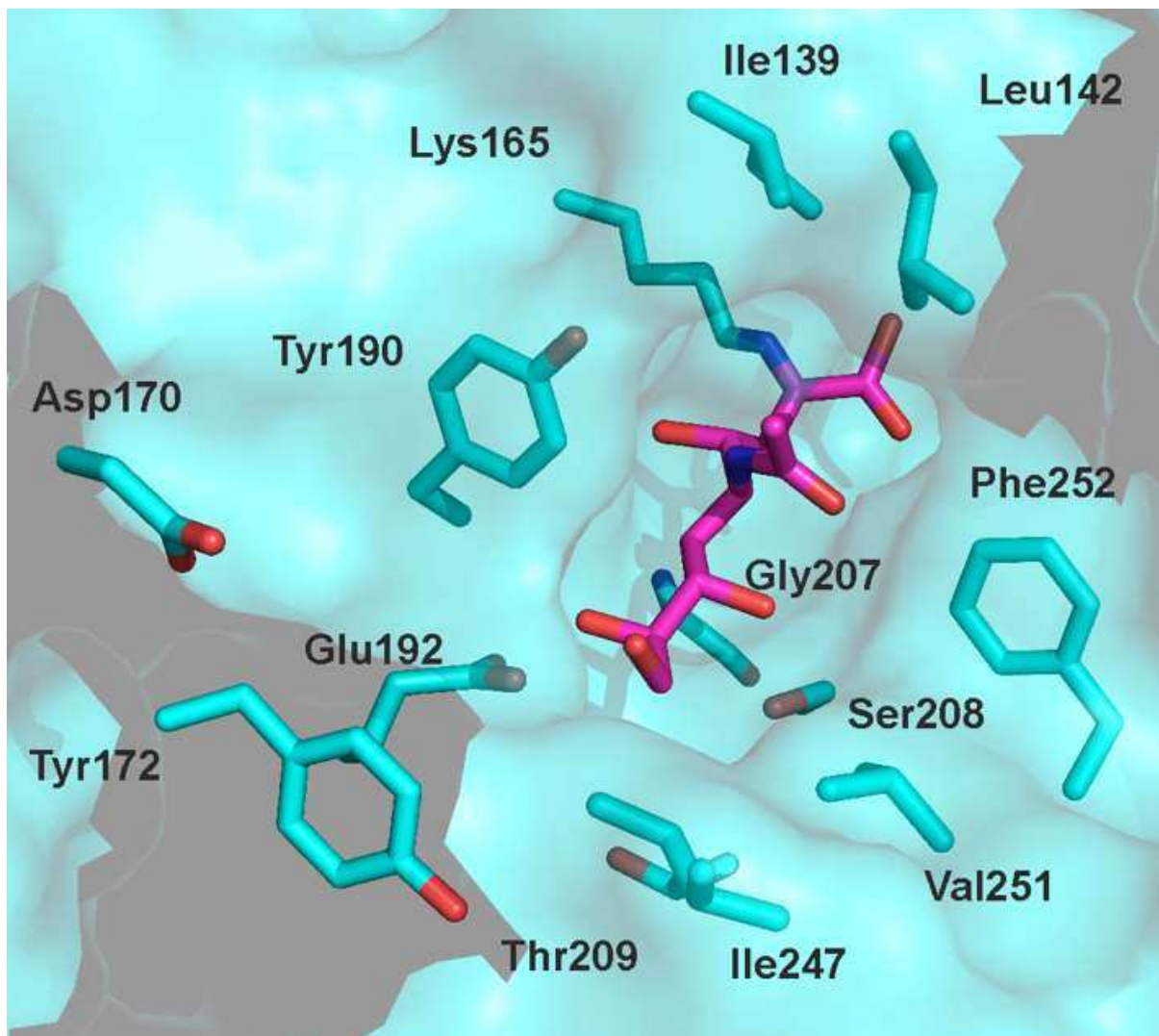


Fig 4

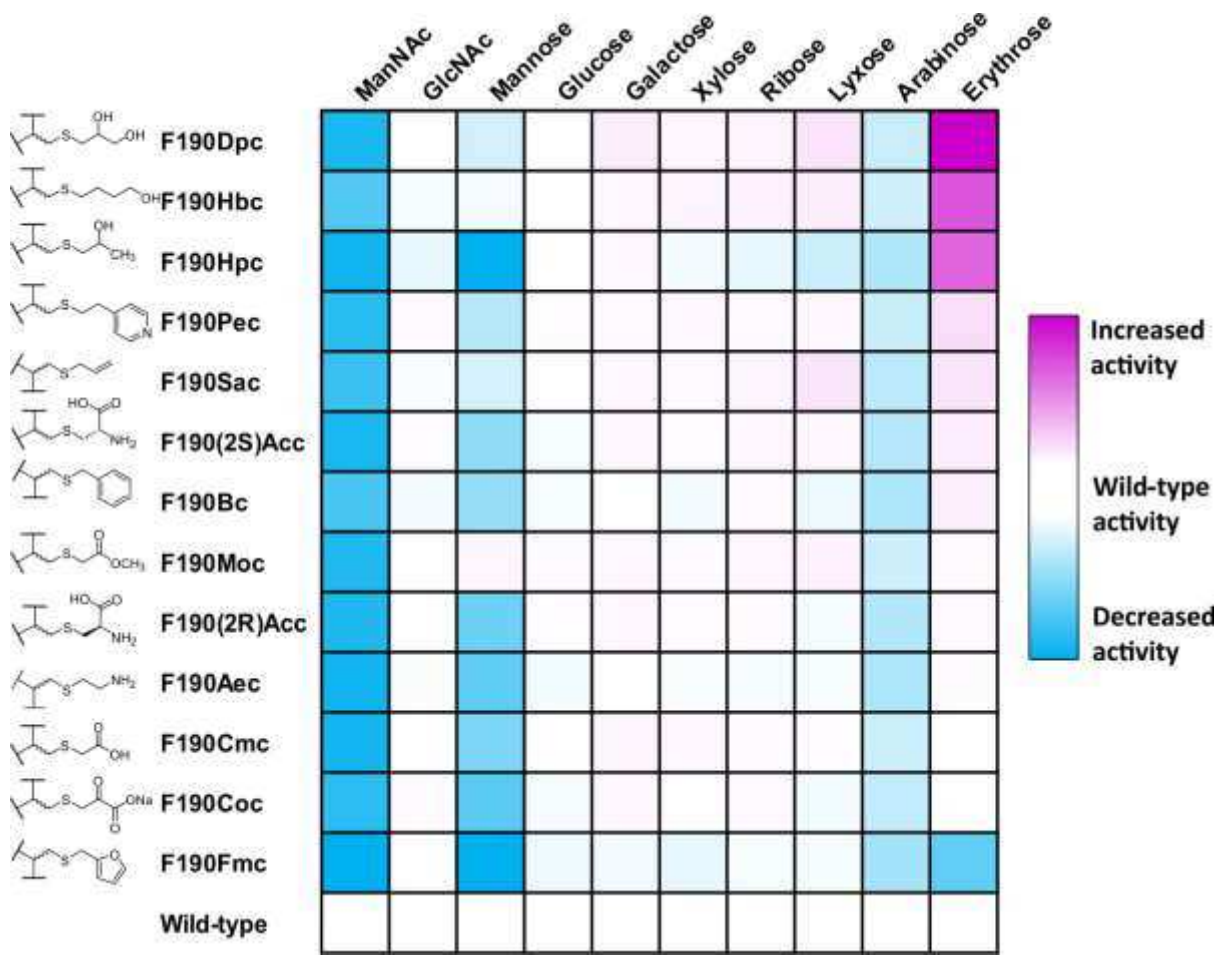
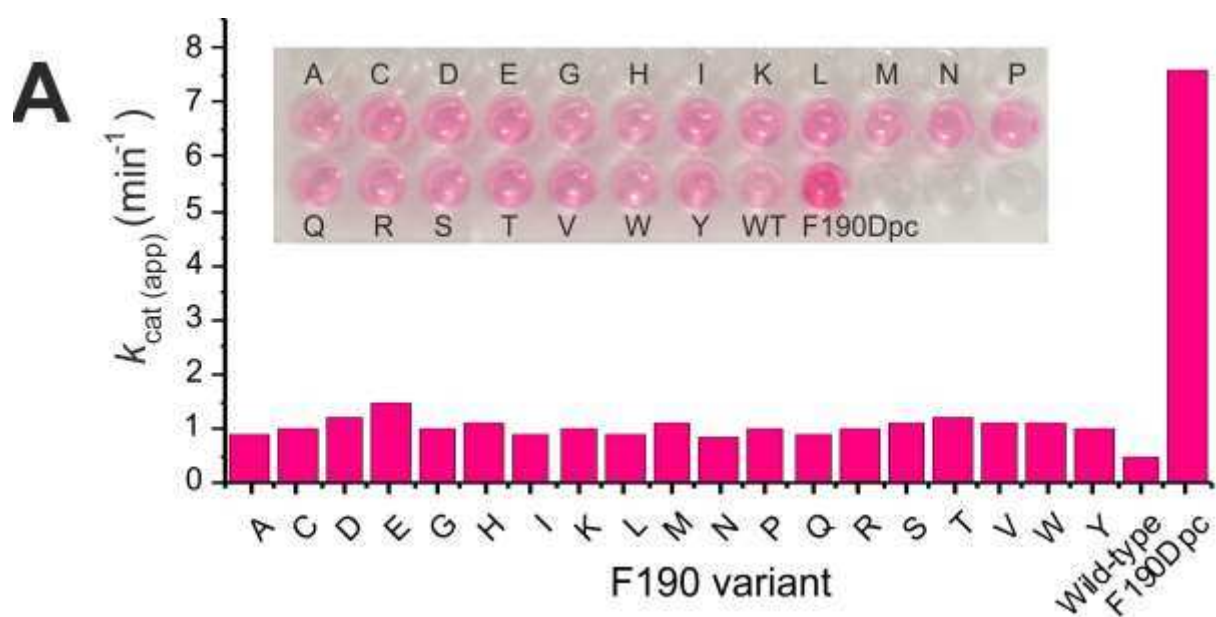


Fig 5



B

F190 Variant	$k_{\text{cat}}^{\text{app}}$ (min^{-1})	$K_{\text{m}}^{\text{app}}$ (mM)	$k_{\text{cat}}^{\text{app}} / K_{\text{m}}^{\text{app}}$ ($\text{min}^{-1} \text{mM}^{-1}$)
A	0.9 ± 0.2	7.8 ± 4.5	0.12
C	1.0 ± 0.16	7.2 ± 2.3	0.14
D	1.2 ± 0.06	2.8 ± 0.45	0.43
E	1.5 ± 0.3	4.7 ± 2.4	0.32
G	1.0 ± 0.34	5.0 ± 4.0	0.20
H	1.1 ± 0.09	4.0 ± 0.82	0.28
I	0.9 ± 0.07	2.9 ± 0.8	0.31
K	1.0 ± 0.05	2.0 ± 0.40	0.50
L	0.9 ± 0.02	2.3 ± 0.26	0.39
M	1.1 ± 0.05	2.0 ± 0.40	0.55
N	0.84 ± 0.07	3.3 ± 0.80	0.25
P	1.0 ± 0.11	4.2 ± 1.2	0.24
Q	0.89 ± 0.05	1.5 ± 0.40	0.6
R	1.0 ± 0.01	1.6 ± 0.08	0.63
S	1.1 ± 0.1	2.7 ± 1.1	0.41
T	1.2 ± 0.03	2.0 ± 0.4	0.6
V	1.1 ± 0.03	1.6 ± 0.3	0.69
W	1.1 ± 0.03	2.4 ± 0.24	0.46
Y	1.0 ± 0.05	1.3 ± 0.3	0.77
Wild-type (F)	0.5 ± 0.05	3.0 ± 0.9	0.17
F190Dpc	7.6 ± 0.56	4.4 ± 0.81	1.7

Fig 6

